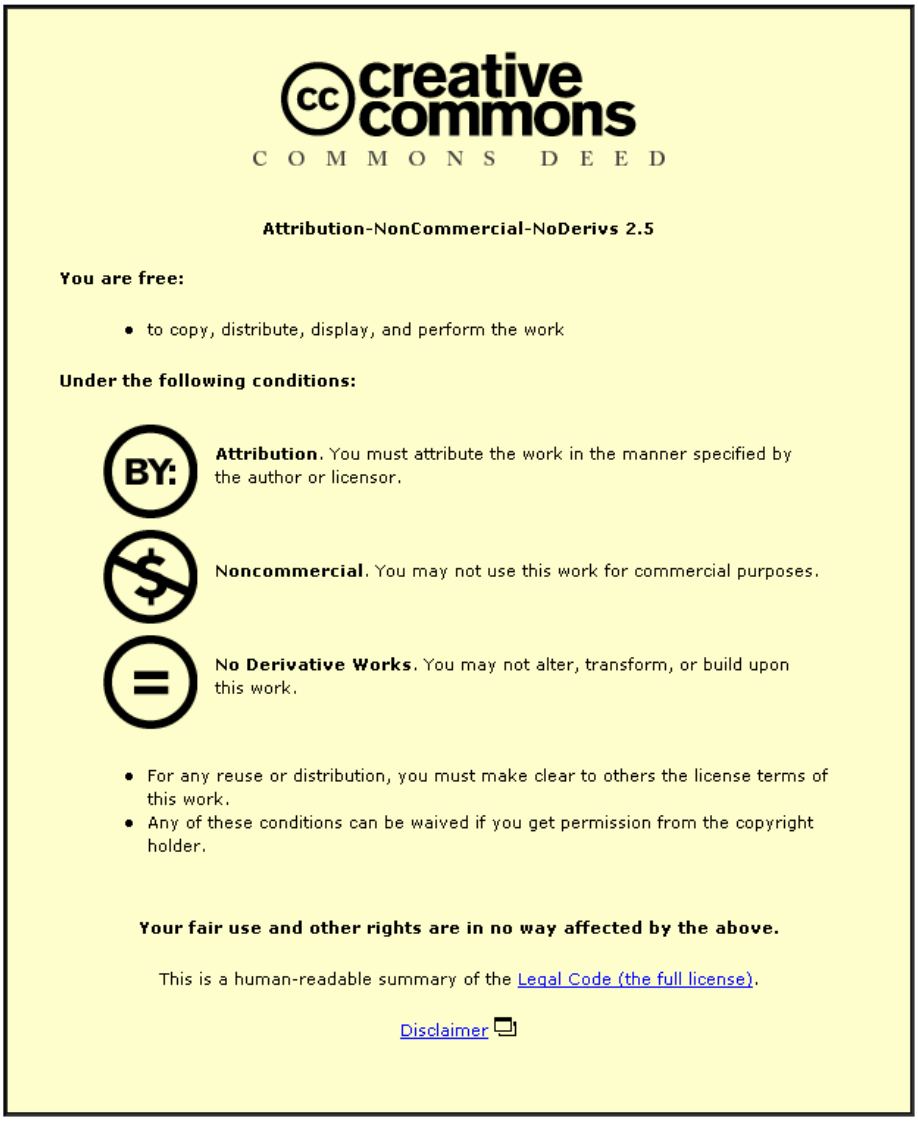

creative commons

COMMONS DEED

Attribution-NonCommercial-NoDerivs 2.5

You are free:

- to copy, distribute, display, and perform the work

Under the following conditions:

BY: **Attribution**. You must attribute the work in the manner specified by the author or licensor.

Noncommercial. You may not use this work for commercial purposes.

No Derivative Works. You may not alter, transform, or build upon this work.

- For any reuse or distribution, you must make clear to others the license terms of this work.
- Any of these conditions can be waived if you get permission from the copyright holder.

Your fair use and other rights are in no way affected by the above.

This is a human-readable summary of the Legal Code (the full license).

Disclaimer

On-line Additions of Aqueous Standards for Calibration of Laser Ablation Inductively Coupled Plasma Mass Spectrometry: Theory and Comparison of Wet and Dry Plasma Conditions

Ciaran O' Connor,[a] Barry L. Sharp[a]* and Peter Evans[b]

[a]*Analytical Atomic Spectroscopy Group, Department of Chemistry, Loughborough University, Loughborough, Leicestershire, LE11 3TU, UK*

**E-mail: b.l.sharp@lboro.ac.uk; Tel: 01509 222572*

[b]*Specialised Techniques, LGC, Queens Road, Teddington, Middlesex, TW11 OLY, UK*

Abstract

This paper describes the theory of on-line additions of aqueous standards for calibration of Laser Ablation Inductively Coupled Plasma Mass Spectrometry (LA-ICP-MS). Establishment of a calibration curve enabled investigation of: fractionation, matrix effects, mass flow ratios, and the relative merits of wet and dry plasma conditions for laser ablation sampling. It was found that a wet plasma was much more tolerant of increased sample loading without reducing plasma robustness, leading to less severe and more constant mutual matrix effects. These findings indicate that the on-line addition of water is the preferred mode of operation for quantification by LA-ICP-MS.

The analytical performance of the method was validated by the analysis of three certified reference materials: National Institute of Standards and Technology (NIST) 612 Trace Elements in Glass, European Reference Material (ERM) 681 Trace Elements in Polyethylene and British Chemical Standards (BCS) No. 387 Nimonic 901 Alloy. Analysis of NIST 612 was performed under both wet and dry plasma conditions, and the correlation with certified elemental concentrations was much

better when a wet plasma was employed. Analyses of ERM 681 and BCS No. 387 were performed under wet plasma conditions, due to its proven advantages. The differences between the found and certified elemental concentrations varied between 1 – 10 % for the majority of elements, for all three certified reference materials.

Introduction

Laser Ablation Inductively Coupled Plasma Mass Spectrometry (LA-ICP-MS) has become the most versatile technique for the direct determination of trace elements in a wide variety of solid sample types. It has particular application for the determination of trace elements in sample types such as metals, rocks, polymers and ceramics, and avoids the risk of contamination associated with complex digestion procedures.

The limitations of LA-ICP-MS are well known; namely elemental fractionation and a lack of certified reference materials (CRMs) for the majority of sample types. 'In house' synthetic standards can be prepared for this purpose, although their preparation is often time consuming and expensive, and they are frequently compromised by in-homogenous distribution of elemental composition. In the absence of solid calibration standards, aqueous calibration standards have been employed for quantification. Such aqueous standards can be ablated directly, with[1] or without[2] the presence of an organic chromophore to improve coupling between the laser and solution, or more commonly they are introduced on-line via a nebuliser and spray chamber in what is referred to as the "dual sample/standard approach".

Dual sample/standard calibration

The dual sample/standard approach, first proposed by Thompson *et al.*,[3] can provide quantitative data in the absence of solid calibration standards. In this calibration approach, the aerosol generated by laser ablation of the target is combined with the aerosol generated by solution nebulisation of an aqueous calibration standard.

The limitation of this approach is the different sample and standard matrices that result in differing atomisation and ionisation characteristics within the ICP. Namely,

ablated particles have larger mean diameters and size distributions than those particles produced by solvent evaporation from a wet aerosol.[4-6] Consequently, these particles are vaporised along an extended region of the ICP, leading to wider ion density distributions along the central channel for LA in comparison to solution nebulisation.[7, 8]

The dual sample/standard approach, using a wet or a dry plasma, requires internal standardisation to compensate for the different mass transport rates of the two sample introduction sources. Consequently, an element of known concentration and homogenous distribution must be present in the sample. However, this may not be as restrictive as at first may seem, since a matrix element of known concentration (from stoichiometry, or previous analysis) is often available.

In its simplest form, dual sample/standard introduction produces a wet plasma, leading to the possibility of spectral interferences such as oxides and hydroxides derived from the use of water as a solvent. In this paper the term "wet" refers to a plasma in which the liquid phase aerosol and vapour phase water are present, i.e. the classical wet plasma produced in solution analysis. Normally, desolvation of the standard aerosol is employed so that it more closely matches the sample aerosol.[9-15] However, the plasma formed in this case is referred to as being "dry", and has a variable composition depending upon the matrix of the ablation target; hence variable sample matrix will produce varied sample loading. In contrast, a wet plasma produces more standardised conditions with a single dominant plasma species i.e. water; thus water dominates the plasma loading and only small perturbations are caused by the sample matrix leading to reduced matrix effects.

Whereas the absence of oxides and hydroxides may be necessary for the accurate determination of isotopic ratios, the standardised plasma conditions offered by employing a wet plasma may be of greater benefit for routine analysis by LA-ICP-MS. Koch *et al.*[16] observed that the $^{65}Cu/^{66}Zn$ ratio from brass using LA-ICP-MS with dry plasma conditions differed to the ratios obtained using wet plasma conditions. This was also confirmed by Boulyga *et al.*[17] who reported that the $^{65}Cu/^{66}Zn$ ratio obtained by LA-ICP-MS using wet plasma conditions, was closer to the ratio obtained with a traditional digest and solution based nebulisation, than using dry plasma

conditions. These differences can probably be attributed to differential fractionation within the ICP, between dry and wet plasma conditions, due to different atomisation and ionisation conditions.

This work develops the theory of the on-line dual sample/standards technique and provides a comparison between the use of wet or dry plasma conditions. A strategy was devised using on-line, multi-point aqueous calibration, allowing the investigation of fractionation, matrix effects and characterisation of a mass flow ratio representing the ratio of mass transport between the two sources.

Theory of On-line Additions

Nomenclature

I = Intensity or ion count rate

C = Concentration

$C_A^L|_0$ = X-axis intercept at I = 0

S = Sensitivity

$\dot{m}$ = Mass flow rate

Superscript

^{S} = Solid or sample

^{L} = Liquid standard

$^{S+L}$ = Solid in the presence of the aqueous standard aerosol

---

Subscript

$_I$ = Internal standard

$_A$ = Analyte

Generally the calibration function for an ICP-MS instrument is written as:

$$I = CS \qquad \textbf{(1)}$$

The sensitivity (*S)* factor can be split into two terms; a *true instrumental sensitivity* term i.e. the response of the ICP-MS instrument per unit mass (strictly speaking molar quantities should be used since these directly represent the number of atoms sampled) of a specified element and a *mass flow rate* term representing the flux of sample or standard. Thus for an analyte in the sample substrate, Equation 1 becomes:

$$I_A^S = \dot{m}_A^S C_A^S S_A^S \qquad \textbf{(2)}$$

Dimensional analysis of Equation 2 is instructive in understanding the meanings of the individual terms, thus:

$$\frac{counts}{s} = \frac{g^S}{s} \times \frac{g_A}{g^S} \times \frac{counts}{g_A} \qquad \textbf{(2b)}$$

Note how the cancellation of dimensions is between, rather than within terms, indicating the inherent separation of sample and analyte quantities.

For on-line additions the overall intensity is the sum of the intensity contributions from the sample and from the standard, in accordance with a standard additions type calibration. Hence:

$$I_A = \dot{m}_A^L S_A^L C_A^L + \dot{m}_A^S S_A^{S+L} C_A^S \qquad \textbf{(3)}$$

Note that two sensitivity terms are present; one, S_A^L , representing the sensitivity of the aqueous calibration curve; and the other, S_A^{S+L}, representing the sensitivity of the on-line additions calibration curve i.e. the sensitivity of the combined solid sample and aqueous standard. Plotting I_A against C_A^L yields a graph as shown in Figure 1, with slope of $\dot{m}_A^L S_A^L$ and intercept of $\dot{m}_A^S S_A^{S+L} C_A^S$.

Extrapolation of the on-line addition curve to $I_A = 0$, and rearrangement of Equation 3, yields the concentration of the analyte in the sample as:

$$C_A^S = -\frac{\dot{m}_A^L}{\dot{m}_A^S} \times \frac{S_A^L}{S_A^{S+L}} \times C_A^L|_0 \qquad \textbf{(4)}$$

$C_A^L|_0$, which is negative, is taken directly from the graph, and it remains to determine the *mass flow ratio*, $\frac{\dot{m}_A^L}{\dot{m}_A^S}$, since the *sensitivity ratio*, $\frac{S_A^L}{S_A^{S+L}}$, can be calculated from the slopes of the two curves. It is this sensitivity ratio that can be used as a direct indicator of mutual matrix effects, i.e. two parallel curves indicate no mutual matrix effects, whereas any divergence or convergence indicates mutual matrix effects are occurring. The mass flow ratio can be determined by performing on-line additions for an internal standard element; hence, Equation 4 can be written as:

$$-\frac{\dot{m}_I^L}{\dot{m}_I^S} = \frac{C_I^S}{\frac{S_I^L}{S_I^{S+L}} \times C_I^L|_0} \qquad \textbf{(5)}$$

Knowing C_I^S, the mass flow ratio can be determined. For this to be useful in solving Equation 4, it is necessary to assume that:

$$\frac{\dot{m}_I^L}{\dot{m}_I^S} = \frac{\dot{m}_A^L}{\dot{m}_A^S} \qquad \textbf{(6)}$$

That is, there is no elemental fractionation between the internal standard element and the analyte, since differing mass flow ratios are a direct measure of elemental fractionation.

Experimental

Instrumentation

A commercially available UP-213 Laser Ablation System (New Wave Research Inc., Huntingdon, Cambridgeshire, UK) operating in the deep UV (213 nm) was employed using He as a carrier gas due to its improved ablation and transport characteristics.[18-20] Figure 2 shows the experimental arrangement used throughout the investigation. The sample aerosol from the LA system was combined with the standard aerosol from a PFA-100 μL Fixed Capillary Nebuliser (Elemental Scientific Inc., Omaha, Nebraska, USA) and custom made cyclonic spray chamber, using a polypropylene 'Y'-piece (Fisher Scientific, Loughborough, Leicestershire, UK). With this arrangement a wet plasma resulted. When a dry plasma was required, the nebuliser and spray chamber was replaced with a MCN-6000 sample introduction system (CETAC Technologies, Omaha, Nebraska, USA) for desolvation of the standard aerosol. The two 1 m, Tygon™, sample introduction lines were combined, using a polypropylene 'Y'-piece, 1 m before the ICP torch. A further cyclonic mixing vessel was placed immediately before the ICP torch. This was placed in the Peltier chamber of the PQ ExCell and was cooled to 5 ^{o}C as in standard operating mode. The gas flow, carrying the combined sample and standard aerosol, was introduced tangentially into this vessel to facilitate further mixing.

A VG PQ ExCell ICP-MS instrument (Thermo Electron Corporation, Winsford, Cheshire, UK) was used throughout the investigation. Optimisation of the torch-box position, lens voltages, and nebuliser gas flow was performed before analysis, with respect to the ^{115}In signal intensity obtained upon nebulisation of a 1 μg L^{-1} solution. A He gas flow of 0.5 L min^{-1} was found to give optimum sensitivity and a good peak shape upon single shot ablation of NIST 612, and importantly had no detrimental effects on the signal intensity obtained upon solution nebulisation when the two sample introduction sources were combined. All optimisation was performed at 1350 W. Table 1 lists the experimental parameters employed. The laser conditions were chosen to represent those typically used in of bulk analysis by LA-ICP-MS.

Sample Preparation

Solid Samples

NIST 612 (National Institute of Standards and Technology, Gaithersburg, Maryland, USA) Trace Elements in Glass was used when performing investigations into laser and plasma variables, due to its certification for a wide variety of trace elements. For method validation, NIST 612 Trace Elements in Glass, European Reference Material (ERM) 681 Trace Elements in Polyethylene and British Chemical Standards (BCS) No. 387 Nimonic 901 Alloy (42 % Nickel, 36 % Iron, 12 % Cr, 6 % Mo and 3 % Ti) were analysed. No sample preparation was performed on these materials, excepting the chemical cleaning of the sample surface with 1 % HNO_3 (Romil Pure Chemistry, Cambridge, Cambridgeshire, UK).

Aqueous Standard Preparation

Aqueous calibration standards, in a 1 % HNO_3 matrix, were prepared by serial dilution of elemental stock solutions (Fisher Scientific, Loughborough, Leicestershire, UK) using 18.2 MΩ cm^{-1} purity water (Elga Lab Water, High Wycombe, Buckinghamshire, UK). These standards contained the following elements: Ti, Cr, Mn, Co, Cu, Sr, Ag, Cd, Ba, Ce, Tl, Pb and U at concentrations 0, 1, 2, 5 and 10 μg L^{-1}.

On-line Additions

The on-line additions involved simultaneous introduction of aqueous calibration standard aerosols by solution nebulisation, with or without desolvation, and a laser ablated sample aerosol. In order to allow the investigation of matrix effects and calculation of the mass flow ratio, multiple calibration standards were used. The whole calibration series was nebulised (with He passing through the ablation cell) to yield a standard calibration curve. Then, ablation of the sample commenced and the aqueous calibration series was repeated, so that simultaneous introduction of sample and standard occurred. This procedure yielded two curves, as shown in Figure 1; one curve representing the contribution from the aqueous calibration standards only; and the other representing the contribution from the aqueous calibration standards in

addition to the laser ablated sample aerosol. Comparison of the slope of the two curves enabled an investigation into the occurrence of mutual matrix effects, as explained above. The mean and standard deviation of the sensitivity ratios obtained from various isotopes (n = 14) was used as an indication of the extent and consistency of matrix effects.

Data were acquired under different ablation and plasma conditions, including: ablation crater diameter and plasma forward power. By increasing crater diameter and keeping the fluence constant, the ablated mass and consequently the sample loading of the plasma was increased. Further, since the fluence remained constant throughout the investigation, the ablation products should remain similar (particle size distribution etc.), leaving sample yield as the sole variable. Crater diameters of 15 – 110 μm were investigated. The effect of plasma robustness on matrix effects was investigated by performing on-line additions under varying ICP forward powers, within the range of 1100 – 1600 W. This investigation was performed using fixed carrier gas flows. Although forward power and injector flow are recognised as being interdependent variables, it was felt that in these experiments changing the Ar/He ratio and hence the transport properties of the delivery systems might introduce too many additional variables. All experiments were performed using both standard solution nebulisation, and solution nebulisation with desolvation to allow a comparison between wet and dry plasma conditions.

Calibration Procedure

Once the optimum ablation and plasma conditions were found, with respect to minimising matrix effects, the reference materials were analysed. First, using on-line simultaneous sample/standard introduction for an internal standard element, a mass flow ratio was calculated. Then, by performing on-line simultaneous sample/standard introduction for the analyte element and applying the mass flow ratio obtained from the internal standard element, C_A^S was calculated from Equation 4.

For NIST 612 Trace Elements in Glass the analysis was performed under wet and dry plasma conditions and the quality of the data compared with the certified elemental

concentrations. Analyses of ERM 681 Polyethylene and BCS No. 387 Nimonic 901 Alloy were performed using wet plasma conditions only.

For analysis using a dry plasma, an ICP forward power of 1500 W was used; whereas, for a wet plasma 1300 W was applied. LA parameters were kept constant throughout the analysis: a fluence of 13 mJ cm^{-2}, a frequency of 20 Hz, an ablation crater diameter of 80 μm and a sample translation rate of 10 μm s^{-1} were employed.

Results and Discussion

Variation in Ablation Crater Diameter

The on-line additions strategy was performed at differing ablated crater diameters i.e. successively introducing more ablated mass into the ICP to increase the sample loading of the plasma. The data obtained are presented in Table 2 and Table 3.

Increasing the ablated crater diameter had the effect of increasing the relative sensitivity above unity, and importantly the standard deviation in the sensitivity ratios obtained. This effect was much more pronounced under dry plasma conditions than under wet plasma conditions as can be seen in Figure 3.

The laser was run at constant fluence, leading to increased mass transport to the ICP with increasing ablated crater diameter; consequently the sample loading of the plasma was increased. Under dry plasma conditions, with higher sample loading it appears that the plasma became less robust, leading to more severe matrix effects. The elements were affected by a less robust ionisation source to different extents (due to properties such as first and second ionisation enthalpy and oxide bond strength etc.). The increased plasma loading manifested itself as an increase in sensitivity ratios, and the standard deviation thereof, across the suite of elements studied.

The degree of variation in the sensitivity ratios with increased sample loading was much more constant under wet plasma conditions. It appears that the presence of water buffered the plasma against the detrimental effects of sample loading on plasma robustness. Importantly, the data indicates that there was no significant change in the extent of oxide formation upon the introduction of the laser ablated aerosol. This is shown by the absence of any significant change in sensitivity upon introduction of the sample aerosol, especially for the oxide forming elements Ce and U. Oxide and hydroxide formation would be expected if less robust plasma conditions existed. The fact that the level of oxides remained constant upon introduction of the sample aerosol again indicates that the presence of water was beneficial in maintaining robust plasma conditions. The best way to detect changes in oxide formation is to monitor the $^{140}Ce^{16}O/^{140}Ce$ ratio; however this was not possible in this case as the ablation of the

NIST glass produces several interfering species at the *m/z* 156. For this reason, the molecular ion $^{238}U^{16}O^{+}$ (*m/z* 254) was monitored as an indicator as to the extent of oxide formation. Under wet plasma conditions there was no increase in the degree of oxide formation for U upon introduction of the ablated aerosol, indicating there was no significant change in plasma robustness. This can be seen in Table 3, wherein the ratio $\%UO^{L}$ / $\%UO^{S+L}$, (representing the degree of UO formation for standard introduction only, divided by the degree of UO formation for simultaneous sample and standard introduction) does not deviate from unity under wet plasma conditions. Under dry plasma conditions this ratio is more erratic and deviations from unity were obtained indicating that the dry plasma was more susceptible to changes in sample loading.

The more constant sensitivity ratios obtained under wet plasma conditions have implications when applying an internal standard element in a calibration by LA-ICP-MS. Using wet plasma conditions, it is more likely that data obtained from an internal standard element will be representative of a larger suite of elements. The mean sensitivity ratio at an ablation crater diameter of 110 μm did not quite follow the trend, but the change was small and is not likely to indicate a true reversal of slope.

Variation in Plasma Forward Power

The on-line additions strategy was performed for varying ICP forward powers, with fixed LA parameters, to determine the effect of forward power on the severity of matrix effects for both wet and dry plasma conditions. The results can be seen in Table 4 and Table 5.

As shown in Figure 4, under wet plasma conditions, the standard deviation of the sensitivity ratios was almost constant with respect to changes in ICP forward power. For dry plasma conditions, the variation in sensitivity ratios, was strongly related to the ICP forward power. This can be explained by differences in plasma robustness i.e. a low ICP forward power and high sample load yielded a less robust plasma, leading to severe matrix effects. As stated above, under wet plasma conditions this effect was much less pronounced, confirming that the presence of water buffered against the detrimental effects of low plasma robustness. Again, the data indicated that the degree

of oxide formation remained constant with varying ICP forward power, upon introduction of the laser ablated aerosol, when wet plasma conditions were employed. This is shown in Table 5 wherein the $\%UO^{L}$ / $\%UO^{S+L}$ is more constantly close to unity than for dry plasma conditions (notwithstanding that the smaller ratios obtained for the dry plasma will lead to greater statistical variation).

The fact that the presence of water alters the fundamental properties of the plasma, such as temperature and electron density is well documented.[21-30] However, the effects of water remain poorly understood, with experimental outcomes often depending upon the exact details of the sample introduction system and the total water flux and vapour/liquid ratio. It was beyond the scope of this investigation to quantify all of these parameters. Generally, plasma energy is consumed in the vaporisation and dissociation processes; however, this energy can be replaced by energy transfer from the outer regions of the plasma into the central channel, and the dissociation products (molecular hydrogen and oxygen) contribute to a local increase in thermal conductivity and heat transfer. The more robust conditions offered by employing a wet plasma have been observed in the present work. The wet plasma was more tolerant of variable sample loading and variable ICP forward powers, evidenced by more constant sensitivity ratios.

Calibration

Method validation was performed on NIST 612 Trace Elements in Glass, ERM 681 Trace Elements in Polyethylene and BCS No. 387 Nimonic 901 Alloy. The uncertainty quoted on all calculated concentrations is based upon the standard error ($S_{y/x}$) associated with the whole calibration curve and is a very robust estimate of the uncertainty associated with each result. Thus, the concentration uncertainties were calculated from the regression line for a signal intensity of $\pm S_{y/x}$.[31] This method ignores the uncertainties in the concentration values, which is justified in the case of the NIST 612 glass, since the relative uncertainties are only 10 % of the LA data values, but not so valid in the case of ERM 681 Polyethylene.

Analysis of NIST 612 Trace Elements in Glass

Co was chosen as an internal standard element for the analysis of NIST 612 Trace Elements in Glass, since it provided a mass flow ratio that was most representative of the other elements under both wet and dry plasma conditions i.e. its mass flow ratio was close to the mean. This indicates that there was little fractionation between Co and the other elements, with the possible exception of Ti (as indicated by differing mass flow ratios). It should be noted that for the analysis of a 'real' sample this data would not be available and it is unlikely that there would be such a choice of internal standard element. However, here, since this data was available, then a selection of the best internal standard was made. LA is no different to any other analytical technique in that prior knowledge of the sample will improve data quality. The optimum ICP forward powers obtained from the previous investigation were employed for the analysis i.e. 1300 W for the wet plasma analysis, although from previous investigation this was not too critical, and 1500 W for the dry plasma analysis. The data obtained can be seen in Table 6 and Table 7.

The results for the mass flow ratios indicate that there was a much greater signal contribution from the aqueous calibration standards than from the laser ablated aerosol. This is highlighted by the large values calculated for the mass flow ratio i.e. the ratio of flux between sample and standard. Values this large are indicative of the small amounts of ablated material transported to the ICP when employing such a LA system. This value means that an analyte concentration of tens of mg kg^{-1} in the solid sample will correspond to a signal intensity equivalent to one μg L^{-1} of analyte in the aqueous calibration standards. This may be disadvantageous in terms of absolute detection limit, but as shown here, limiting the plasma loading is beneficial for obtaining good quantitative data.

The analysis proved a lot more successful when wet plasma conditions were used. Generally, the agreement between the calculated and certified concentrations was much closer under the wet plasma conditions. Under wet plasma conditions, the majority of elements quantified were within 1 – 10 % of the certified values. One exception was Ti, for which poorer data was obtained, but no explanation for this is available.

The matrix effects were less severe and less variable between elements when using a wet rather than a dry plasma, as a direct result, the mass flow ratios calculated were less elementally variable, indicating that they were subject to less fractionation. This simplifies the choice of an internal standard, since it is more likely that the chosen element will be more representative of the set. For this reason, more accurate data can be obtained from the on-line additions approach when wet plasma conditions are employed. This is shown in Figures 5 and 6, wherein a better correlation between the calculated elemental concentrations and certified elemental concentrations was obtained under wet plasma conditions, shown by a slope close to 1 obtained when using a wet plasma and a slope well below 1 when using a dry plasma ($R^2_{Wet} = 0.89$ vs. $R^2_{Dry} = 0.60$).

Analysis of ERM No. 681 Trace Elements in Polyethylene

Analysis of ERM No. 681 Polyethylene was undertaken as an example of a typical polymer sample. For this analysis Cd was chosen as an internal standard element, due to it being in the middle of the mass range investigated. The data obtained are shown in Table 8.

The analysis proved successful in that excellent agreement with the certified concentrations was obtained. When using Cd as an internal standard element, agreement within 2 % of the certified concentrations was obtained for the quantification of Cr and Pb. Mass flow ratios were much smaller for the polyethylene than those obtained for the NIST glass. Since the output from the nebuliser generally remained constant for all three analyses, then the change in mass flow ratio must have been due to a large difference in the ablated mass transported to the plasma. The results indicate that much more polymer sample was transported, most likely due to increased coupling between the laser beam and the polymer.

Analysis of BCS No. 387 Nimonic 901 Alloy

Analysis of BCS No. 387 Nimonic 901 Alloy was undertaken as an example of a typical metal alloy sample. For this analysis Cu was chosen as an internal standard element. The data obtained are shown in Table 9.

Using Cu as an internal standard, the analysis proved successful in the quantification of Co and Pb, and good agreement with the certified concentration was obtained. The quantification of Mn was less successful. This was due to the fact that the certified concentration of Mn was very high in the reference material, producing a signal intensity above the linear range of the ICP-MS detector (especially when combined with the signal intensity from the aqueous calibration standards). This gave erroneous calibration data, leading to an inaccurate quantification. Mass flow ratios were similar to those obtained for the polymer sample, again indicating that there was an increased transport of metal sample to the plasma in comparison to the glass.

Conclusions

Although dry plasma conditions may be beneficial when performing isotope ratio measurements by LA-ICP-MS due to reduced oxides and hydroxides, it has been shown that a wet plasma is more advantageous for routine analysis. The findings indicate that the on-line additions of water is the preferred mode of operation for quantification by LA-ICP-MS. Employing a wet plasma produces more standardised plasma conditions and buffers against the detrimental effects of sample loading and reduced plasma robustness. Furthermore, the exclusion of a desolvation system results in faster analysis time (due to reduced sample uptake, wash-in and wash-out times) and less expense (due to reduced analysis time, energy and gas requirements).

The theory presented in this paper has enabled differentiation between "sensitivity" and mass flow. The calculation of a mass flow ratio is useful not only for calibration, but also as a measure of the relative flux between two sample introduction sources. The mass flow ratios reported indicate the very small amounts of material that are transported to the plasma from the ablation site when compared to the quantities introduced by a standard nebuliser and spray chamber. It has been shown that different samples can yield highly different mass flow ratios, related to the optical and physico-chemical properties of the sample. Differences in the mass flow ratios between elements are a direct indication of the occurrence and extent of elemental fractionation.

This paper has shown that on-line additions of aqueous calibration standards without desolvation can produce rapid and 'fit for purpose' quantitative data in the absence of a CRM. The ability of this method to make such determinations has particular relevance with the introduction of the Restriction of the use of certain Hazardous Substances (RoHS) and Waste Electrical and Electronic Equipment (WEEE) Directives.

The practical aspects of multi-point on-line additions calibration may make it more useful for method development than practical analysis, (as a pre-cursor to a single point calibration by normal internal standardisation) especially since it requires a large sample area of homogenous analyte and internal standard distribution and

typically a ten minute time for sample analysis. For example, the method could be performed on a CRM to investigate fractionation and matrix effects, aiding the choice of internal standard (if a choice is available), before subsequent single point calibration on the real sample.

Acknowledgements

This work was performed with financial backing from the Valid Analytical Measurements Program (VAM). The authors would like to express their gratitude to Thermo Electron Corporation (Winsford, Cheshire, UK) for provision of the VG PQ ExCell ICP-MS instrument and LGC (Teddington, Middlesex, UK) for provision of the UP-213 LA system.

References

1 F. Boue-Bigne, B. J. Masters, J. S. Crighton and B. L. Sharp, *J. Anal. At. Spectrom.*, 1999, **14**, 1665.

2 D. Günther, R. Frischknecht, H. J. Muschenborn and C. A. Heinrich, *Fresenius' J. Anal. Chem*, 1997, **359**, 390.

3 M. Thompson, S. Chenery and L. Brett, *J. Anal. At. Spectrom.*, 1989, **4**, 11.

4 P. Arrowsmith and S. K. Hughes, *Appl. Spectrosc.*, 1988, **42**, 1231.

5 P. M. Outridge, W. Doherty and D. C. Gregoire, *Spectrochim. Acta, Part B*, 1996, **51**, 1451.

6 P. M. Outridge, W. Doherty and D. C. Gregoire, *Spectrochim. Acta, Part B*, 1997, **52**, 2093.

7 I. Rodushkin, M. D. Axelsson, D. Malinovsky and D. C. Baxter, *J. Anal. At. Spectrom.*, 2002, **17**, 1223.

8 I. Rodushkin, M. D. Axelsson, D. Malinovsky and D. C. Baxter, *J. Anal. At. Spectrom.*, 2002, **17**, 1231.

9 D. Günther, H. Cousin, B. Magyar and I. Leopold, *J. Anal. At. Spectrom.*, 1997, **12**, 165.

10 J. J. Leach, L. A. Allen, D. B. Aeschliman and R. S. Houk, *Anal. Chem.*, 1999, **71**, 440.

11 J. S. Becker, C. Pickhardt and H. J. Dietze, *J. Anal. At. Spectrom.*, 2001, **16**, 603.

12 C. Pickhardt, J. S. Becker and H. J. Dietze, *Fresenius' J. Anal. Chem*, 2000, **368**, 173.

13 C. Pickhardt and J. S. Becker, *Fresenius' J. Anal. Chem*, 2001, **370**, 534.

14 L. Halicz and D. Gunther, *J. Anal. At. Spectrom.*, 2004, **19**, 1539.

15 A. G. Coedo, I. Padilla and M. T. Dorado, *Appl. Spectrosc.*, 2004, **58**, 1481.

16 J. Koch, I. Feldmann, N. Jakubowski and K. Niemax, *Spectrochim. Acta, Part B*, 2002, **57**, 975.

17 S. F. Boulyga, C. Pickhardt and J. S. Becker, *At. Spectrosc.*, 2004, **25**, 53.

18 S. M. Eggins, L. P. J. Kinsley and J. M. G. Shelley, *Appl. Surf. Sci.*, 1998, **129**, 278.

19 D. Günther and C. A. Heinrich, *J. Anal. At. Spectrom.*, 1999, **14**, 1363.

20 I. Horn and D. Günther, *Appl. Surf. Sci.*, 2003, **207**, 144.

21 S. E. Long, R. D. Snook and R. F. Browner, *Spectrochim. Acta, Part B*, 1985, **40**, 553.

22 S. E. Long and R. F. Browner, *Spectrochim. Acta, Part B*, 1986, **41**, 639.

23 B. L. Caughlin and M. W. Blades, *Spectrochim. Acta, Part B*, 1987, **42**, 353.

24 J. Farino, J. R. Miller, D. D. Smith and R. F. Browner, *Anal. Chem.*, 1987, **59**, 2303.

25 S. E. Long and R. F. Browner, *Spectrochim. Acta, Part B*, 1988, **43**, 1461.

26 P. E. Walters and C. A. Barnardt, *Spectrochim. Acta, Part B*, 1988, **43**, 325.

27 R. F. Browner and S. E. Long, *Spectrochim. Acta, Part B*, 1989, **44**, 831.

28 D. E. Nixon, *J. Anal. At. Spectrom.*, 1990, **5**, 531.

29 J. W. Olesik and S. J. Den, *Spectrochim. Acta, Part B*, 1990, **45**, 731.

30 I. Novotny, J. C. Farinas, J. L. Wan, E. Poussel and J. M. Mermet, *Spectrochim. Acta, Part B*, 1996, **51**, 1517.

31 J. N. Miller and J. C. Miller, *Statistics and Chemometrics for Analytical Chemistry*, 4th Ed., Pearson Education Limited, Harlow, U.K., 2000.

Tables and Figures

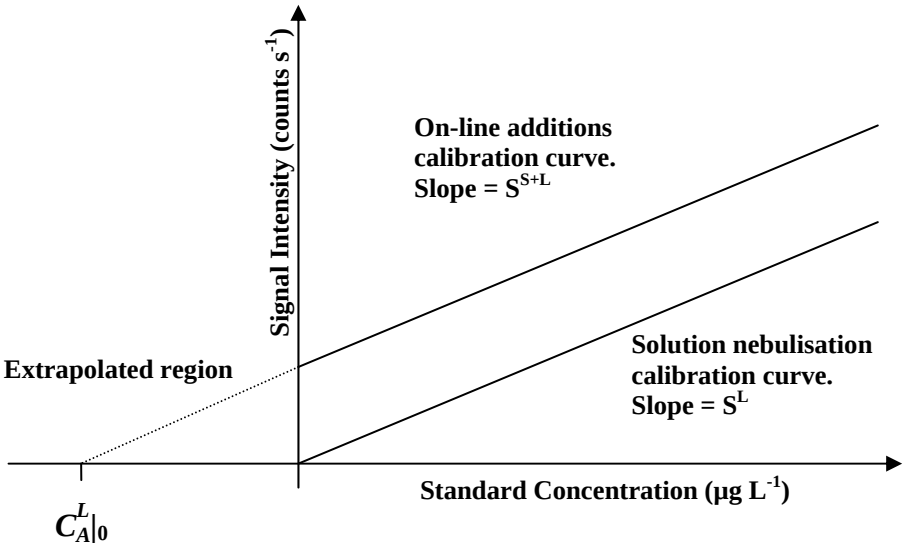

Figure 1 A representation of the curves obtained by aqueous calibration and on-line additions calibration. In this simple scenario there are no mutual matrix effects, as indicated by the parallel curves, hence $S^{L} = S^{S+L}$.

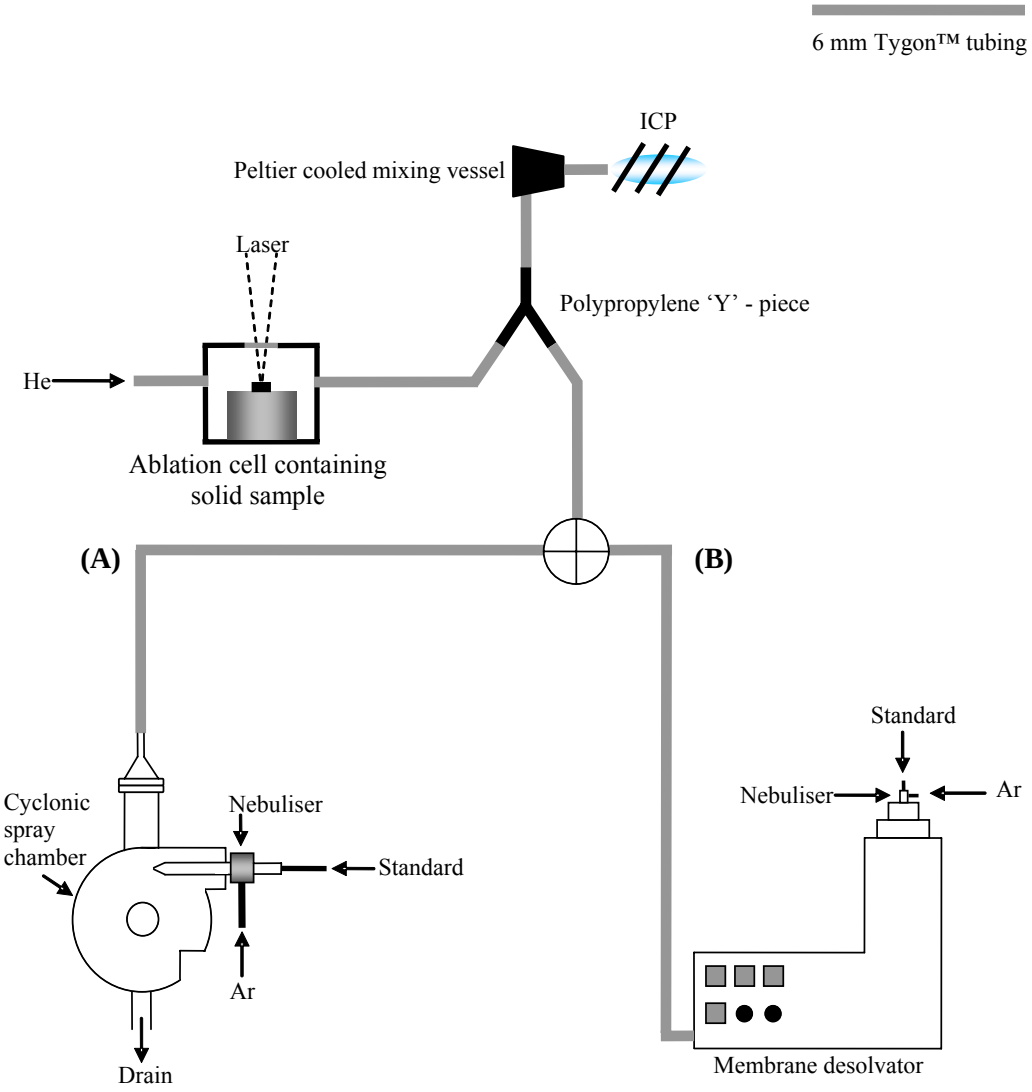

Figure 2 The two different experimental setups employed: (A) aqueous standards introduced by standard solution nebulisation to produce a wet standard aerosol and (B) introducing the standard aerosol by solution nebulisation with desolvation to produce a dry standard aerosol.

Table 1 Experimental parameters used in the investigation.

Laser Ablation System	
Type	Solid state Nd:YAG, UP-213
Wavelength	213 nm
Pulse duration	4 ns
Fluence	13 mJ cm^{-2}
Repetition rate	20 Hz
Sampling strategy	Raster
Spot diameter	15 – 110 μm
Solid samples	NIST 612 Trace Elements in Glass ERM Trace Elements in Polyethylene 681

	BCS No. 387 Nimonic 901 Alloy
Sample translation rate	10 μm s^{-1}
He gas flow	0.5 L min^{-1}
Solution Nebulisation	
Nebuliser	PFA-100 μL Fixed Capillary
Ar carrier gas flow	0.95 L min^{-1}
Spray chamber	Custom cyclonic
Desolvation System	
Type	MCN-6000
Ar carrier gas flow	0.95 L min^{-1}
Sweep gas flow	3.80 L min^{-1}
Spray chamber temperature	75 ^{o}C
Desolvator temperature	160 ^{o}C
ICP-MS	
Type	VG PQ ExCell
Auxiliary gas flow	0.80 L min^{-1}
Cooling gas flow	12.00 L min^{-1}
Peltier chamber temperature	5 ^{o}C
Plasma RF power	1100 – 1600 W
Isotopes monitored	^{47}Ti, ^{52}Cr, ^{55}Mn, ^{59}Co, ^{65}Cu, ^{88}Sr, ^{107}Ag, ^{111}Cd, ^{137}Ba, ^{140}Ce, $^{140}Ce^{16}O$, ^{205}Tl, ^{206}Pb, ^{208}Pb, ^{238}U, $^{238}U^{16}O$,
Acquisition mode	Peak hopping
Detector mode	Dual range
Channels per peak	1
Dwell time	100 ms
No. of sweeps	100
No. of replicates	3

Table 2 Standard deviation and mean of sensitivity ratios obtained under varying ablated crater diameters, during the analysis of NIST 612.

Ablated crater diameter (μm)	**Standard deviation of sensitivity ratios (n=14)**		**Mean of sensitivity ratios (n=14)**	
	Wet	**Dry**	**Wet**	**Dry**
15	0.005	0.012	1.030	1.041
30	0.009	0.024	1.038	1.023
55	0.022	0.036	1.065	1.119
80	0.029	0.072	1.144	1.139
110	0.040	0.106	1.008	1.286

Table 3 Degrees of UO^+ formation using a wet and dry plasma, with and without the presence of a laser ablated aerosol for varying ablated crater diameters. The ratio % UO^L / % UO^{S+L} thus represents any changes in the degree of oxide formation upon introduction of the ablated aerosol.

Ablated crater diameter (µm)	**Wet plasma oxide analysis**			**Dry plasma oxide analysis**		
	% UO^L	**% UO^{S+L}**	**% UO^L / % UO^{S+L}**	**% UO^L**	**% UO^{S+L}**	**% UO^L / % UO^{S+L}**
15	1.40	1.37	1.02	0.08	0.08	1.00
30	1.41	1.50	0.94	0.09	0.07	1.29
55	1.39	1.39	1.00	0.1	0.08	1.25
80	1.43	1.36	1.05	0.08	0.08	1.00
110	1.41	1.40	1.01	0.09	0.08	1.13

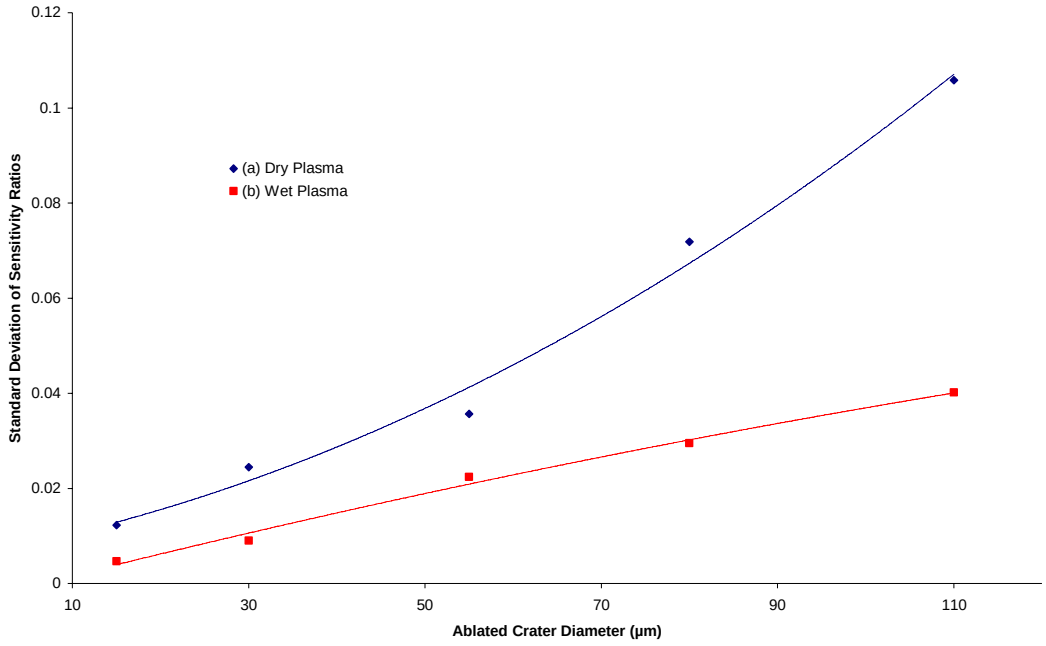

Figure 3 Standard deviation (n=14) of sensitivity ratios obtained with differing ablated crater diameter, during the analysis of NIST 612, under (a) dry and (b) wet plasma conditions.

Table 4 Standard deviation and mean of sensitivity ratios obtained under varying ICP forward power, during the analysis of NIST 612.

ICP forward power (W)	Standard deviation of sensitivity ratios (n=14)		Mean of sensitivity ratios (n=14)	
	Wet	Dry	Wet	Dry
1100	0.050	0.159	0.990	1.152
1200	0.038	0.080	1.124	1.073
1300	0.011	0.064	1.27	1.214
1400	0.030	0.053	1.109	1.408
1500	0.035	0.052	0.962	1.274
1600	0.031	0.066	1.002	0.935

Table 5 Degrees of UO^+ formation using a wet and dry plasma of varying forward power, with and without the presence of a laser ablated aerosol. The ratio % UO^L / % UO^{S+L} thus represents any changes in the degree of oxide formation upon introduction of the ablated aerosol.

ICP forward power (W)	Wet plasma oxide analysis			Dry plasma oxide analysis		
	% UO^L	% UO^{S+L}	% UO^L / % UO^{S+L}	% UO^L	% UO^{S+L}	% UO^L / % UO^{S+L}
1100	7.21	7.92	0.91	1.47	1.25	1.18
1200	1.95	1.71	1.14	0.49	0.45	1.09
1300	1.52	1.52	1.00	0.15	0.22	0.67
1400	1.41	1.53	0.92	0.08	0.07	1.09
1500	1.30	1.18	1.10	0.05	0.05	1.05
1600	1.42	1.30	1.09	0.05	0.08	0.66

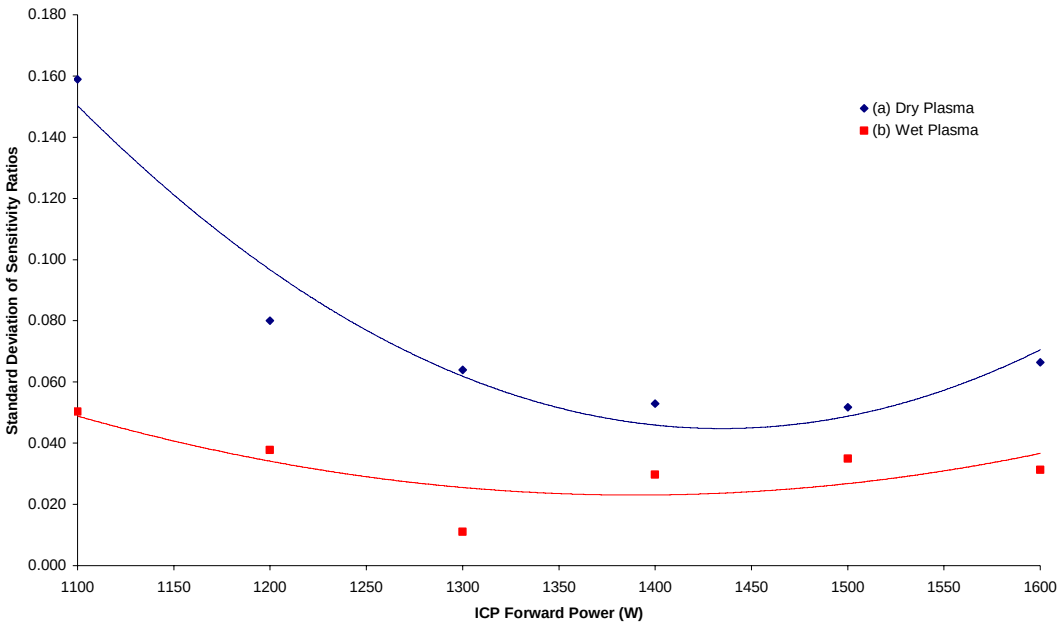

Figure 4 Standard deviation (n=14) of sensitivity ratios obtained with differing ICP forward power, during the analysis of NIST 612, under both (a) dry and (b) wet plasma conditions.

Table 6 Data for NIST 612 showing the certified elemental concentration, calculated mass flow ratio and calculated elemental concentration using Co as an internal standard, performed under wet plasma conditions with constant LA parameters.

Isotope	Certified concentration with associated uncertainty (mg kg^{-1})	Mass flow ratio	Calculated concentration with associated uncertainty (mg kg^{-1})	% Recovery
^{47}Ti	50.1 ± 0.8	10982	63.3 ± 4.8	126
^{52}Cr	Not certified	-	36.4 ± 2.5	-
^{55}Mn	39.6 ± 0.8	14697	37.4 ± 1.9	94
^{59}Co	**35.5 ± 1.2**	**13888**	**Internal standard**	-
^{65}Cu	37.7 ± 0.9	16170	32.4 ± 2.6	86
^{88}Sr	78.4 ± 0.2	14896	73.1 ± 4.7	93
^{107}Ag	22 ± 0.3	13092	23.3 ± 3.5	106
^{111}Cd	Not certified	-	20.6 ± 0.9	-
^{137}Ba	41 ± Not quoted	17044	33.4 ± 1.2	81
^{140}Ce	39 ± Not quoted	13731	39.4 ± 2.6	101
^{205}Tl	15.7 ± 0.3	14386	15.2 ± 1.4	97
^{206}Pb	38.57 ± 0.2	14338	37.4 ± 1.6	97
^{208}Pb	38.57 ± 0.2	13863	38.6 ± 1.5	100
^{238}U	37.38 ± 0.08	14042	37.0 ± 4.0	101
Mean	**-**	**14294**	**-**	**98**

Table 7 Data for NIST 612 showing the certified elemental concentration, calculated mass flow ratio and calculated elemental concentration using Co as an internal standard, performed under dry plasma conditions with constant LA parameters.

Isotope	Certified concentration with associated uncertainty (mg kg^{-1})	Mass flow ratio	Calculated concentration with associated uncertainty (mg kg^{-1})	% Recovery
^{47}Ti	50.1 ± 0.8	21055	30.7 ± 3.0	61
^{52}Cr	Not certified	-	40.1 ± 3.2	-
^{55}Mn	39.6 ± 0.8	16193	34.4 ± 3.0	87
^{59}Co	**35.5 ± 1.2**	**14074**	**Internal standard**	-
^{65}Cu	37.7 ± 0.9	11999	44.2 ± 7.1	117
^{88}Sr	78.4 ± 0.2	21065	52.4 ± 4.8	67
^{107}Ag	22 ± 0.3	11248	27.5 ± 3.7	125
^{111}Cd	Not certified	-	30.0 ± 1.8	-
^{137}Ba	41 ± Not quoted	19549	29.5 ± 3.0	72
^{140}Ce	39 ± Not quoted	15618	35.1 ± 3.0	90
^{205}Tl	15.7 ± 0.3	9667	22.9 ± 1.6	146
^{206}Pb	38.57 ± 0.2	10258	30.7 ± 9.5	80
^{208}Pb	38.57 ± 0.2	9869	32.2 ± 12.3	83

^{238}U	37.38 ± 0.08	11336	23.8 ± 6.3	64
Mean	**-**	**14328**	**-**	**90**

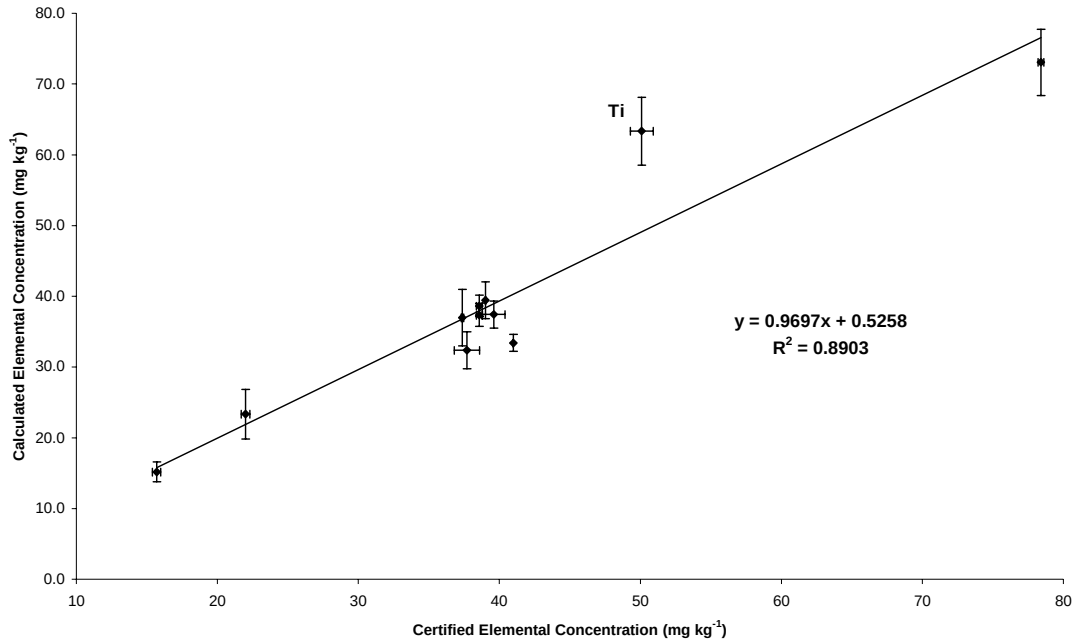

Figure 5 The correlation between the calculated elemental concentrations and the certified elemental concentrations, using Co as an internal standard element, under wet plasma conditions for NIST 612.

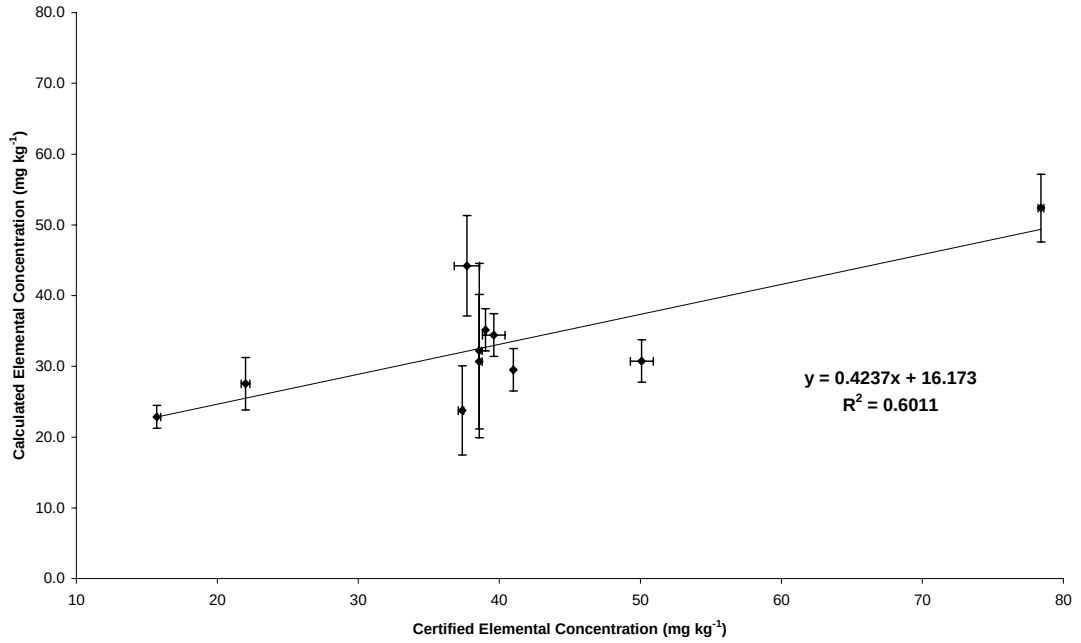

Figure 6 The correlation between the calculated elemental concentrations and the certified elemental concentrations, using Co as an internal standard element, under dry plasma conditions for NIST 612.

Table 8 Data for ERM 681 Trace Elements in Polyethylene showing the certified elemental concentration, calculated mass flow ratio, and calculated elemental concentration using Cd as an internal standard, performed under wet plasma conditions with constant LA parameters.

Isotope	Certified concentration with associated uncertainty (mg kg^{-1})	Mass flow ratio	Calculated concentration with associated uncertainty (mg kg^{-1})	% Recovery
^{52}Cr	17.7 ± 0.6	4974	17.5 ± 3.5	99
^{111}Cd	**21.7 ± 0.7**	**4910**	**Internal standard**	**-**
^{206}Pb	13.8 ± 0.7	4813	14.1 ± 0.48	102
^{208}Pb	13.8 ± 0.7	4869	13.9 ± 0.43	101
Mean	**-**	**4892**	**-**	**101**

Table 9 Data for BCS 387 Nimonic 901 Alloy showing the certified elemental concentration, calculated mass flow ratio and calculated elemental concentration using Cu as an internal standard and performed under wet plasma conditions with constant LA parameters.

Isotope	Certified concentration with associated uncertainty (mg kg^{-1})	Mass flow ratio	Calculated concentration with associated uncertainty (mg kg^{-1})	% Recovery
^{55}Mn	250 ± Not quoted	4575	193 ± 4	77
^{59}Co	200 ± Not quoted	4703	198 ± 7	99
^{65}Cu	**76 ± Not quoted**	**4660**	**Internal standard**	**-**
^{206}Pb	0.8 ± Not quoted	5107	0.73 ± 0.23	91
^{208}Pb	0.8 ± Not quoted	4933	0.75 ± 0.19	95
Mean	**-**	**4796**	**-**	**91**